A Lagrangian stochastic model for rod orientation in turbulent flows

Lorenzo Campana, Mireille Bossy, Jean Minier

A Lagrangian stochastic model for rod orientation in turbulent flows

Lorenzo Campana[1], Mireille Bossy[1] and Jean Pierre Minier[2]

[1]Université Côte d'Azur, Inria, France

lorenzo.campana@inria.fr, mireille.bossy@inria.fr

[2]EDF R&D, MFEE, Chatou, France

jean-pierre.minier@edf.fr

Keywords: Turbulent flow, anisotropic particles, stochastic modelling

Abstract

Suspension of anisotropic particles can be found in various applications, e.g. industrial manufacturing processes or natural phenomena (micro-organism locomotion, ice crystal formation in clouds). Microscopic ellipsoidal bodies suspended in a turbulent fluid flow rotate in response to the velocity gradient of the flow. Understanding their orientation is important since it can affect the optical or rheological properties of the suspension (e.g. polymeric fluids). In this work, the orientation dynamics of rod-like tracer particles, i.e. long ellipsoidal particles (in the limit to infinity of the aspect-ratio) is studied. The size of the rod is assumed smaller than the Kolmogorov length scale but sufficiently large that its Brownian motion need not be considered. As a result, the local flow around a particle can be considered as inertia-free and Stokes flow solutions can be used to relate particle rotational dynamics to the local velocity gradient tensor $A_{ij} = \partial u_i/\partial x_j$. The orientation of a rod is described as the normalized solution of the linear ordinary differential equation for the separation vector $\boldsymbol{R}_{12}$ between two fluid tracers. Separation evolves under the action of the velocity gradient tensor. Simultaneously, a re-normalization procedure $\boldsymbol{R}_{12}/\|\boldsymbol{R}_{12}\|$ is introduced to obtain the unit-vector $\boldsymbol{p}$ aligned with the rod. In this frame, the rod orientation is described by a Lagrangian stochastic model, assuming that cumulative effects of the velocity gradient tensor on the observation time interval fluctuate with a Gaussian distribution. Indeed, cumulative velocity gradient fluctuations are here represented by a white-noise tensor such that it preserves the incompressibility condition. Large observation timescale (overall objective of the work) justifies the Gaussian distribution hypotheses, with a decorrelation timescale equal to the Kolmogorov one τ_η. Finally, the Lagrangian stochastic model is tested in the case of homogeneous isotropic turbulence.

Introduction

Turbulent flows with suspended particles of non spherical shape are a common occurrence in many industrial and natural processes. Industrial processes include pulp making and papermaking (Lundell et al. 2011), as well as soot emission from combustion processes (Moffet and Prather 2009). Natural processes include the dispersion of pollen species in the atmosphere (Sabban and van Hout 2011), the dynamics of icy clouds (Heymsfield 1977), and the cycle of plankton such as diatoms (Musielak et al. 2009). In many of these applications, the flow is highly turbulent and has an effect on the rotational dynamics, alignment trends and correlations of anisotropic particles (such as fibers, discs or more general shapes). In a turbulent flow, a small ellipsoidal particle rotates in response to the velocity gradients tensor along its Lagrangian trajectory. Because these Lagrangian velocity gradients are controlled by the small scales, they are similar in many different turbulent flows and have been the focus of extensive study (Meneveau 2011).

The earliest investigation into the motion of non-spherical particles in a carrier fluid is that of Jeffery (1922). For the special case of an axis-symmetric ellipsoid, he derived the evolution equation for the orientation vector as function of the local velocity gradient tensor. In turbulent flows the velocity gradient tensor $A_{ij} = \partial u_i/\partial x_j$ fluctuates and is dominated by small scale motions of the order of Kolmogorov length scale l_η. Much work has focused in rod-like particles whose size is smaller than the l_η. Studies of the orientation dynamics of such particles in turbulent flows have included those of Shin and Koch (2005) and Pumir and Wilkinson (2011) using isotropic turbulence data from direct numerical simulation (DNS), those of Zhang et al. (2001) and Mortensen et al. (2008) for particles in channel flow turbulence using DNS. In many numerical studies, Lagrangian tracking is most often used to determine the particle trajectories and simultaneous time integration of the Jeffery equation along the trajectory leads to predictions of the particles' orientation dynamics. Generic properties of the orientation dynamics, such as the variance of the fluctuating orientation vector or its alignment trends may also be studied by making certain assumptions about the Lagrangian evolution of the carrier fluid's velocity gradient, in particular about its symmetric and skew-symmetric parts, the strain tensor $S_{ij} = (A_{ij} + A_{ji})/2$ and the rotation tensor $\Omega_{ij} = (A_{ij} - A_{ji})/2$.

A number of theoretical studies have been based on the assumption that these flow variables obey isotropic Gaussian statistics, e.g. are the result of linear Ornstein-Uhlenbeck processes (e.g. see Brunk et al. (1998); Pumir and Wilkinson (2011); Wilkinson and Kennard (2012) and Vincenzi (2013)).

For small tracers particles whose size is smaller than the Kolmogorov scale, the local flow around the particle can be considered to be inertia-free and Stokes flow solutions can be used to relate the rotational dynamics of the particles to the local velocity gradient. To understand the dynamics of ellipsoidal particles in turbulence, there are needs to extend the understanding of the Lagrangian statistics of the velocity gradient tensor, and to include the orientational dynamics, resulting from the integrating Jeffery's equation Jeffery (1922) along the particle trajectory. This is a challenging problem, both because of the complexity of statistically quantifying the particle orientation with respect to the velocity gradient tensor. In this frame, the rod orientation is described by a Lagrangian stochastic model, assuming that cumulative effect of the velocity gradient tensor on the observation time interval fluctuate with a Gaussian distribution. Indeed, cumulative velocity gradient fluctuations are here represented by a white-noise tensor such that it preserves the incompressibility condition.

The Lagrangian stochastic model involves three timescales: the Kolmogorov timescale τ_η, the Lagrangian integral timescale of the fluid T_L and the integration timescale Δt. The first two timescales are physical characteristic timescales. The third one, Δt, represents the 'observation' time-scale. Large observation timescale, such as pump clogging (objective of the modeling) justifies the Gaussian distribution hypotheses, with a decorrelation timescale equal to the Kolmogorov one τ_η. Besides, the development of both model and suitable numerical scheme for a large integration time steps, for the stochastic differential equation associated, is a difficult task to address for the separation equation. In this context the focus on the orientation information only is a crucial point. This paper presents some advances in modeling of rod orientation in the context of large observation time-scale simulations and results are reproduced in the context of isotropic homogeneous turbulence.

Equations of motions

Generally speaking, the equation of motion for a rod-like particle (ellipsoid in the limit of infinity aspect-ratio see Fig. 1) in a turbulent velocity field $\boldsymbol{u}(\boldsymbol{r}, t)$ is considered. The rod is assumed to be naturally buoyant and smaller than the smallest length scale characterizing fluid motion, i.e. the Kolmogorov length l_η, but sufficiently large that their Brownian motion do not need be considered. The motion of the rod or "tumbling rate" is determined by the particle orientation and the velocity gradient tensor (as a particular case of the general Jeffery's equation (Jeffery 1922)):

$$\dot{p}_i = \Omega_{ij} p_j + S_{ij} p_j - p_i p_k S_{kl} p_l \tag{1}$$

where $\boldsymbol{p}$ is a unit director along the symmetric axis of the particle, and S_{ij} and Ω_{ij} are the symmetric and skew-symmetric parts of the velocity gradient tensor, respectively. However,
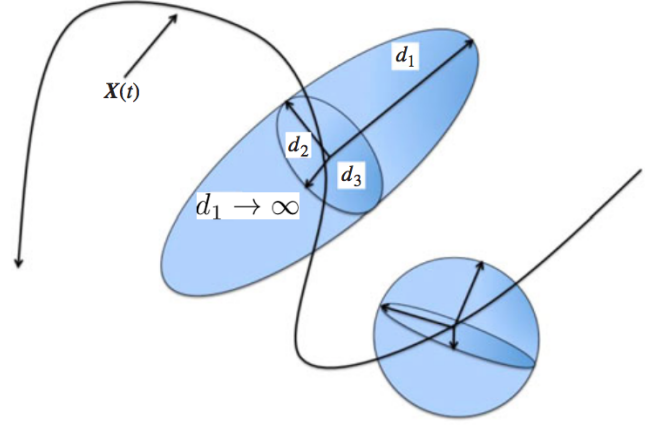

Figure 1: (Colour online) Typical ellipsoidal shape of a fluid element along the turbulent trajectory. The fluid element center of mass $\boldsymbol{X}(t)$ is supposed to follow the evolution of the fluid particle and the deformation is governed by the statistics of the fluid velocity gradients along the trajectory, $\partial_i u_j(\boldsymbol{X}(t), t)$. The fluid element is always assumed of ellipsoidal shape with the three semi-axes ordered as $d_1 \geqslant d_2 \geqslant d_3$. The rod-like particle is described by taking $d_1 \to \infty$. This figure is adapted from Biferale et al. (2014).

this approach leads to a non-linear equation that in the framework of stochastic modeling is difficult to deal with. The same dynamics can be solved by considering a linear equation for the separation of two fluid particles, particularly, the equation of motion has been derived considering the dynamics of two fluid tracers described by the vector $\boldsymbol{R}_{12}$ and eventually normalizing the solution.

In more detail, the separation vector $\boldsymbol{R}_{12} = \boldsymbol{R}_1 - \boldsymbol{R}_2$ between two fluid particles with trajectories $\boldsymbol{R}_n(t) = \boldsymbol{R}(t; \boldsymbol{r}_n)$ passing at $t = 0$ through the points $\boldsymbol{r}_n$ satisfies the equation

$$\dot{\boldsymbol{R}}_{12}(t) = \boldsymbol{v}(\boldsymbol{R}_1, t) - \boldsymbol{v}(\boldsymbol{R}_2, t). \tag{2}$$

In the rest of the paper the subscript $\boldsymbol{R}_{12}$ is replaced by $\boldsymbol{R}$. Considering an incompressible fluid flow where the particles generally separate. In smooth velocity field, for separation $\boldsymbol{R}$ much smaller than the viscous scale of turbulence $l \ll l_\eta$, i.e. the so-called Batchelor regime (Batchelor 1959), the velocity difference between two fluid particles can be expressed as $\boldsymbol{v}(\boldsymbol{R}_1, t) - \boldsymbol{v}(\boldsymbol{R}_2, t) \approx A_{ij}(t)\boldsymbol{R}$ with the Lagrangian strain matrix $A_{ij} = \partial u_i / \partial x_j (R_2(t), t)$. In this regime, Eq. (2) simplifies to the ordinary differential equation

$$\dot{\boldsymbol{R}}(t) = A_{ij}(t)\boldsymbol{R}(t) \tag{3}$$

leading to the linear solution

$$\boldsymbol{R}(t) = W_{ij}(t)\boldsymbol{R}(0) \tag{4}$$

where W_{ij} is evolution matrix or the deformation gradient tensor that characterizes the distortion withstand to the fluid element. The evolution matrix provides a Lagrangian description of the fluid stretching. In other words, for three-dimensional flows, this process can be visualized by considering a sphere that is distorted into a tri-axial ellipsoid ad it is stretched by the flow (see Fig. 1). This means that passive vectors along with thin rods-like become preferentially

aligned with the longest principal axis of the ellipsoid, and at long times approach (after $10\tau_\eta$) perfect alignment with the eigenvector corresponding to the maximum stretching has been studied by Ni et al. (2014).

The general solution for the three dimensional case is determined by products of random matrices. The evolution matrix W_{ij} may be written as

$$
\begin{aligned}
W_{ij}(t) &= \mathcal{T} \exp\Big[\int_0^t A_{ij}(s)ds \Big] \\
&= \sum_{n=0}^\infty \int_0^t A_{ij}(s_n)ds_n \cdots \int_0^{s_3} A_{ij}(s_3)ds_2 \int_0^{s_2} A_{ij}(s_2)ds_1
\end{aligned}
\tag{5}
$$

This time-order exponential form ($\mathcal{T}$), in general, is not very useful for the direct computation except the particular case of a short correlated strain (see sec. Stochastic model for the orientation). The basic idea of the present approach, relies on the result that, in almost realization of the strain gradient tensor, the matrix $1/t \ln W_{ij}W_{ji}$ stabilizes as $t \to \infty$ (see Falkovich et al. (2001) for details). To give some intuitive insight, as already mentioned, considering some fluid volume, like a sphere, which evolves into an elongated ellipsoid at later time. As time increases, the ellipsoid is more and more elongated; furthermore the long time evolution of Eq. (3) is characterized by the following result

$$
\lambda_L = \lim_{t \to \infty} \frac{1}{t} \ln\Big(\frac{|\boldsymbol{R}(t)|}{|\boldsymbol{R}(0)|} \Big)
\tag{6}
$$

which for large t tends with probability one to the largest Lyapunov exponent λ_L (finite value), governing the chaotic properties of the particles trajectories in the turbulent flow. In this way it is possible to solve the rod-like orientation through a linear ordinary differential equation Eq. (3); where the initial conditions are $W_{ij}(0) = I$ (identity matrix) and $\boldsymbol{R}(0) = \boldsymbol{p}(0)$. The solution for rod orientation in Eq. (1) is obtained by normalizing the solution of Eq. (3):

$$
\boldsymbol{p}(t) = \frac{\boldsymbol{R}(t)}{\|\boldsymbol{R}(t)\|}.
\tag{7}
$$

Stochastic model for the orientation

The evolution of $\boldsymbol{p}$ depends upon the velocity gradient tensor $A_{ij}(t)$, therefore a stochastic model for it is presented. Other Lagrangian stochastic model are present in literature, but so far this description has been always investigated in the framework of direct numerical simulations (DNS). Gaussian processes have been proposed for the velocity gradient statistics. For instance, Pumir and Wilkinson (2011) and Vincenzi (2013) have considered an Ornstein-Uhlenbeck process for A_{ij} with a different correlation time scale for the symmetric and skew-symmetric parts. This is more realistic, since it is known that in turbulence the correlation time scale for the rotation rate is significantly longer than that the strain rate. Otherwise, more refined model for the velocity gradient has been obtained by Chevillard and Meneveau (2006), introducing the RFDA model, which overcomes the Gaussian description, predicting a variety of local, statistical, geometric

and anomalous scaling properties of 3-D turbulence. It is important to mention as a reference, the work of Chevillard and Meneveau (2013); which examines in very detail the orientation dynamics of the anisotropic particle in isotropic homogeneous turbulence, using both DNS and different stochastic models. In this framework it is important to underline that these models are tested in a DNS context, or rather, they have been developed for an observation time of the order of the Kolmogorov timescale ($\tau \simeq \tau_\eta$).

The solution of the differential equation such as Eq. (3) with a stochastic input A_{ij} is given by Eq. (5) with the matrix $W_{ij}(t)$ involving stochastic integrands over the time. The case of a short correlated velocity gradient tensor (Kraichnan 1968) allows for a complete solution. More specifically, when the observation time of the dynamics is much larger than the correlation time of the velocity gradient tensor, i.e. $t \gg \tau_\eta$, W_{ij} may be viewed as a continuous product of independent random matrix. Under this assumption, the instantaneous velocity gradient tensor can be decomposed in two contributions: mean field and fluctuations

$$
A_{ij}\big(\boldsymbol{X}(t,\omega),t\big) = \big\langle \partial_i u_j\big(\boldsymbol{X}(t,\omega),t\big)\big\rangle + \xi_{ij}(t,\omega)
\tag{8}
$$

where the $\langle\cdot\rangle$ means the ensemble average and $\xi_{ij}(t,\omega)$ is a white-noise that can be rewritten as $dF_{ij}(t,\omega) = \xi_{ij}(t,\omega)dt$.

This stochastic forcing (fluctuation) is of the form $dF_{ij} = b_{ijkl}dW_{kl}$, where dW_{kl} represent a Wiener process, i.e $\langle W_{ij}\rangle = 0$ and $\langle dW_{ij}dW_{kl}\rangle = \delta_{ik}\delta_{jl}dt$ leading to,

$$
\langle dF_{ij}dF_{kl}\rangle = b_{ijmn}b_{mnkl}dt
\tag{9}
$$

Incompressibility, isotropy and parity invariance impose the form of the fourth-order tensor b_{ijkl},

$$
b_{ijkl} = b_1\delta_{ij}\delta_{kl} + b_2\delta_{ik}\delta_{jl} + b_3\delta_{il}\delta_{jk}.
\tag{10}
$$

with the coefficients $b_1 = (-\sqrt{3}/3)/\tau_\eta^2$, $b_2 = 0.5(\sqrt{3} + \sqrt{5})/\tau_\eta^2$ and $b_3 = 0.5(\sqrt{3} - \sqrt{5})/\tau_\eta^2$ which depend exclusively on the Kolmogorov time scale τ_η (see Johnson and Meneveau (2016) for details).

Now, replacing the decomposition for A_{ij} into the rods' orientation Eq. (3), it is possible to re-formulate the stochastic differential equation (SDE)

$$
dR_i(t) = \langle A_{ij}\rangle R_j dt + dF_{ij} \circ R_j
\tag{11}
$$

interpreted in the Stratonovich form ($\circ$). The natural form for a direct calculation of the SDE is the Itô form, so applying the transformation from Stratonovich to Itô the SDE in the index notation becomes

$$
\begin{aligned}
dR_i =& \Big(\bar{a}_{ii} + \frac{1}{2}\big((b_1 + b_2 + b_3)^2 + 2b_1^2\big)\Big)R_i dt \\
&+ \sum_{j=1}^3 \bar{a}_{ij}R_j(1 - \delta_{ij})dt \\
&+ \Big((b_2 + b_3)dW_{ii} + b_1\sum_{j=1}^3 dW_{jj}\Big)R_i \\
&+ (b_2 + b_3)\sum_{j=1}^3 R_j(1 - \delta_{ij})dW_{ij}
\end{aligned}
\tag{12}
$$

where $\bar{a}_{ij}$ are the elements of $\langle A_{ij} \rangle$ and dW_{ij} is a matrix composed by nine independent Brownian motion. Here, the repeated index is not an implicit summation and δ_{ij} is the Kronecker's symbol. To attain the complete description of the rod's orientation $\boldsymbol{p}$ the SDE is coupled with the normalization procedure, as outlined in the Eq. (7).

It is worth to notice that, when the observation time-step Δt becomes smaller with respect to the Kolmogorov inner time scale τ_η the model for the orientation is no longer valid. This constraint reflects the argument that on a large enough observation time scale (meaning precisely $\Delta t \gg \tau_\eta$), the stochastic model for the orientation is coherent with the physical description of the Lagrangian stochastic model. In particular, it should be stressed that there is a strong interplay between the physical aspects of the model (which leads to a formulation in terms of SDE) and the numerical aspects of the practical simulations as also has been remarked by Minier et al. (2001).

Results and Discussion

This section presents some results obtained from the numerical simulations of the Lagrangian stochastic model described by Eq. (12) and Eq. (7). The model has been performed using a numerical integration scheme based on splitting algorithm, which solves the symmetric and skew-symmetric part of the velocity gradient tensor separately (Campana et al. N.D.). The validation has been restricted to the homogeneous isotropic turbulent (HIT) case, so that the mean velocity gradient tensor is assumed to be zero $\left(\langle A_{ij} \rangle = 0 \right)$. As discussed above, the validation of the model has to be performed for an integration time-step bigger than the Kolmogorov one. Three simulations have been performed: varying the value of the ratio between the observation timescale and the Kolmogorov time scale (the setup for three different *cases* are detailed in Tab. 1). Independent sample of rods have been initialized at time zero, imposing to each of them a uniform distribution on the unit sphere (U(S^2)) for the three *cases*. In the context of HIT, due to the hypotheses of homogeneity and isotropy of the fluid field, the rod orientation vector should remain uniformly distributed on the unit sphere. Firstly, results are presented in the Cartesian coordinate system. The whole sample of orientation vectors $\boldsymbol{p}$ remain, for long time simulation, distributed on the unit sphere as showed in Fig. 2. Regarding the first and second moments of the orientation vector (p_1, p_2, p_3), the Tab. 2 presents measures of the error of mean and variance of the stochastic process evaluating at final time. The empirical mean of any generic moments is denoted as

$$\langle f(\boldsymbol{p}) \rangle_{MC} = \frac{1}{N_p} \sum_{\text{sample}} f(\boldsymbol{p}_{simualtions}) \qquad (13)$$

and the error is usually decomposed in two contributions: the bias part due to the integration scheme and the Monte Carlo error due to the size of sample as,

$$\mathbb{E}\left(\mathbb{E}[\bar{f}(\boldsymbol{p})] - \langle f(\boldsymbol{p}) \rangle_{MC} \right)^2 = \mathcal{O}\left(\Delta t^{2\alpha} \right) + \mathcal{O}\left(\frac{\mathbb{V}ar(f(\boldsymbol{p}))}{N_p} \right) \qquad (14)$$
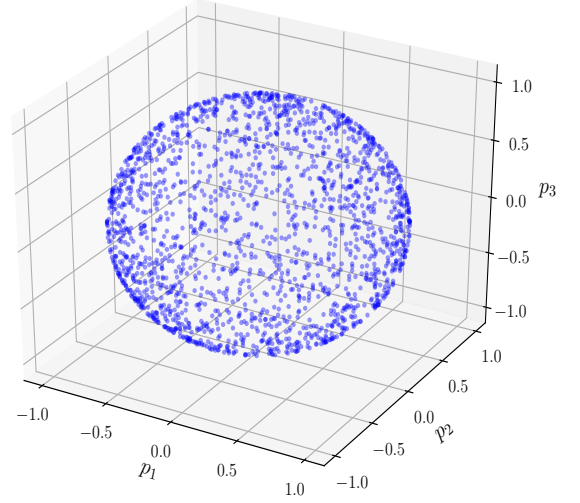

Figure 2: (Colour online) Sample orientation vector evaluated at finale time ($T = 10^3$) distributed on the sphere with a number of iterations 10^5 for the *case 3*.

Setup	Δt	τ/τ_k	N_p	T	$I.d$
Case 1	0.01	1	10^5	10^3	U(S^2)
Case 2	0.1	10	10^5	10^3	U(S^2)
Case 3	1	100	10^5	10^3	U(S^2)

Table 1: Summary of the simulations performed for the Lagrangian stochastic model. For each cases the parameters are referred to: the time-step (Δ), the ratio between the observation and Kolmogorov timescales (τ/τ_k), the numbers of particles used to performed the Monte Carlo (MC) simulations (N_p), the final time (T) and the initial distribution imposed ($I.d$).

The values of the errors are listed in Tab. 2; these are small and of the same order for the three values of the integration time-step Δt. The explanation of this last result relies into the fact that, analyzing the two sources of error, it appears that the total error is dominated by the Monte Carlo approximation, even for the large integration time-step. In Fig. 3 is presented the time evolution of the mean and variance of the rod orientation vector. Both of the mean (see Fig. 3a) and variance (see Fig. 3b) account for the ergodicity of the simulated process. This fact is of main importance regarding the construction of the model (Eq. 6), as discussed above. In fact, the mean oscillates around zero (which is the exact value) for the three component of the orientation vector $\boldsymbol{p}$ (see Fig. 3a) with an error (Tab. 2) that is produced only by the MC simulations for the three *cases*. Similar remarks can be done looking the variance (see Fig. 3b), in this case the value of the components of $\boldsymbol{p}$ fluctuating around the exact value of 1/3 for each of them (Tab. 2).

To complete the description of the numerical results and to have, at the same time, a more physical characterization of the model itself, the results on the empirical probability distribution function ($p.d.f$) are presented. To analyze the
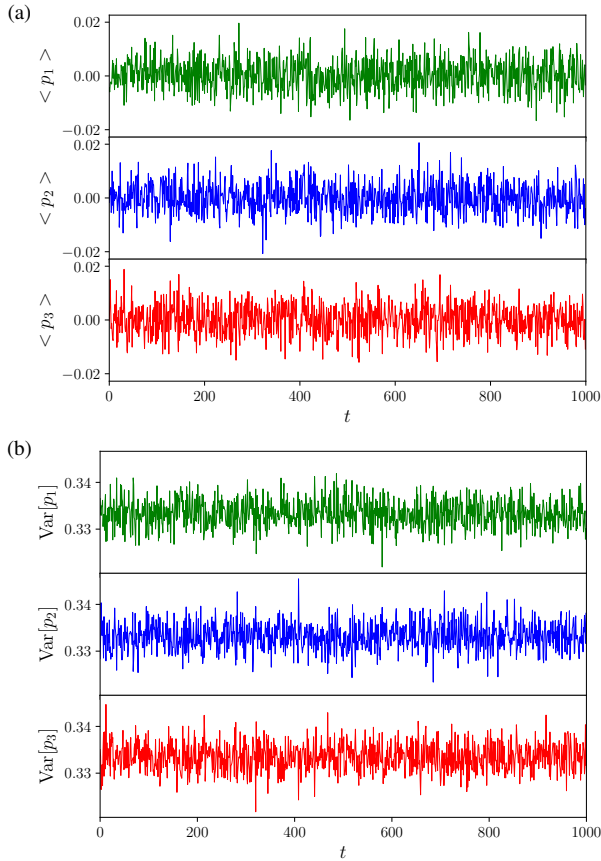
Figure 3: (Colour online) Mean (a) and variance (b) for the three component of the orientation vector $\boldsymbol{p}$ as a function of time, obtained for the *case 3*.

Error	Case 1	Case 2	Case 3
	0.00157	0.00360	0.00089
$\left\lvert \mathbb{E}[p_i] - \langle p_i \rangle_{MC} \right\rvert$	0.00113	0.00005	0.00046
	0.00028	0.00019	0.00172
	0.00060	0.00019	0.00092
$\left\lvert \mathbb{E}[p_i^2] - \langle p_i^2 \rangle_{MC} \right\rvert$	0.00079	0.00021	0.00117
	0.00138	0.00005	0.00211
$\left\lvert \mathbb{E}[g] - \langle g \rangle_{MC} \right\rvert$	0.00005	0.00023	0.00023

Table 2: Estimation of the weak error for the first, second moment and the function $g = g(p_1, p_2, p_3) = p_1 p_2 p_3$. The p_i indicates the exact value, the computed one. The table is organized as following: the error for the mean and variance is computed for each coordinates in order $i = 1, 2, 3$.

orientation dynamics on a non-spherical particle, it is convenient to move from Cartesian coordinates (p_1, p_2, p_3) to spherical coordinates (r, φ, θ) according to the usual transformations

$$r = \sqrt{p_1^2 + p_2^2 + p_3^2},$$

$$\varphi = \arctan\left(\sqrt{p_1^2 + p_2^2}/p_3\right), \quad (15)$$

$$\theta = \arctan(p_2/p_1)$$

with $r \geqslant 0$, $0 \leqslant \varphi \leqslant \pi$ and $0 \leqslant \theta \leqslant 2\pi$. In Fig. 4 are presented the marginal distributions for the two spherical angles: the Fig. 4a and Fig. 4b) show respectively the empirical $pdf(\varphi)$ and $pdf(\theta)$ for the three cases. The three corresponding curves are all in good agreement with the theoretical marginals $p.d.f$:

$$p.d.f(\theta)_{th} = \frac{1}{4\pi} \int_0^\pi \sin \varphi d\varphi = \frac{1}{2\pi}$$

$$(16)$$

$$p.d.f(\varphi)_{th} = \frac{1}{4\pi} \int_0^{2\pi} \sin \varphi d\theta = \frac{1}{2} \sin \varphi.$$

Finally, on account of the unitary length of the orientation vector $\|\boldsymbol{p}\|$ ($r = 1$), the empirical joint probability density function of the orientation must take the form of $p.d.f(\varphi, \theta)$ in spherical coordinates. It is showed in Fig. 5 and its two-dimensional projection Fig. 6. This empirical $p.d.f(\varphi, \theta)$ has been obtained through the use a Gaussian smoothing kernel that wrings the surface near the boundaries of the plots. It appears that the empirical joint $p.d.f$ is in agreement with the theoretical one,

$$p.d.f(\varphi, \theta)_{th} = \frac{1}{4\pi} \sin \varphi. \quad (17)$$

Conclusions

In this study, the rod orientation is described by a Lagrangian stochastic model using dedicated splitting scheme for time integration along large observation time-scale. The cumulative effects of the velocity gradient tensor are assumed fluctuating with a Gaussian distribution with short-time correlations. A new stochastic differential equation (SDE), which describes the separation between two fluid particles, has been proposed. This SDE coupled with a renormalization procedure provides the description of the rod's orientation. The model have been tested numerically in the HIT case and three reference time-scale orders have been examined, showing a good agreement between theoretical and empirical, both for the marginal and joint probability density function expressed in spherical coordinates. This preliminary study serves as a base to go further both on the modeling and the numerical development.

Acknowledgments

Figure 6: (Colour online) Projected empirical joint P.d.f in spherical coordinates produces with the *case 3*.
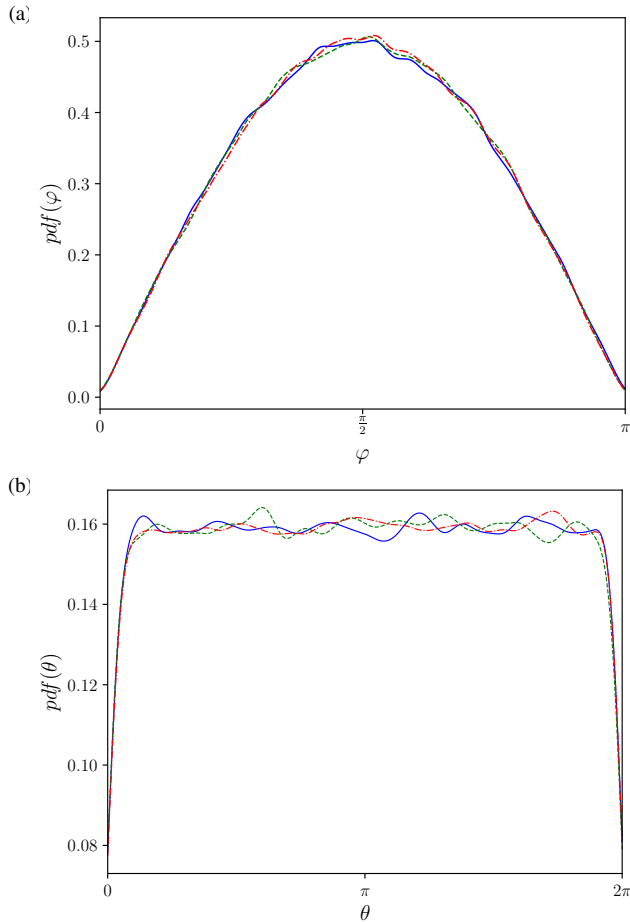
Figure 4: (Colour online) P.d.f of the angle φ in (a) and θ in (b) in the spherical coordinates system. Results from *case 1* (blue solid line), *case 2* (green dashed line) and *case 3* (red dot-dashed line).
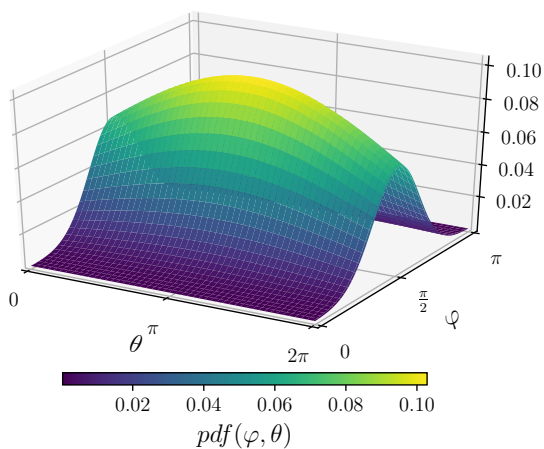

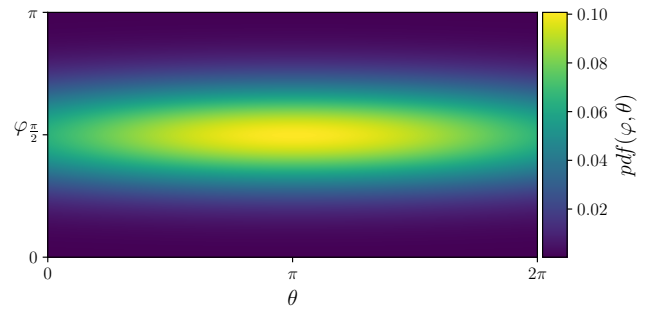Figure 5: (Colour Online) Empirical joint P.d.f in spherical coordinates produces with the *case 3*.

References

George K Batchelor. Small-scale variation of convected quantities like temperature in turbulent fluid part 1. general discussion and the case of small conductivity. *Journal of Fluid Mechanics*, 5(1):113–133, 1959.

Luca Biferale, Charles Meneveau, and Roberto Verzicco. Deformation statistics of sub-kolmogorov-scale ellipsoidal neutrally buoyant drops in isotropic turbulence. *Journal of fluid mechanics*, 754:184–207, 2014.

Brett K Brunk, Donald L Koch, and Leonard W Lion. Observations of coagulation in isotropic turbulence. *Journal of fluid mechanics*, 371:81–107, 1998.

Lorenzo Campana, Mireille Bossy, Minier Jean Pierre, and Christophe Henry. Numerical scheme for a lagrangian stochastic model describing rods orientation. unpublished, N.D.

Laurent Chevillard and Charles Meneveau. Lagrangian dynamics and statistical geometric structure of turbulence. *Physical review letters*, 97(17):174501, 2006.

Laurent Chevillard and Charles Meneveau. Orientation dynamics of small, triaxial–ellipsoidal particles in isotropic turbulence. *Journal of Fluid Mechanics*, 737:571–596, 2013.

G Falkovich, K Gawedzki, and M Vergassola. Particles and fields in fluid turbulence. *Reviews of modern Physics*, 73(4): 913, 2001.

Andrew J Heymsfield. Precipitation development in stratiform ice clouds: A microphysical and dynamical study. *Journal of the Atmospheric Sciences*, 34(2):367–381, 1977.

George Barker Jeffery. The motion of ellipsoidal particles immersed in a viscous fluid. *Proc. R. Soc. Lond. A*, 102(715): 161–179, 1922.

Perry L Johnson and Charles Meneveau. A closure for lagrangian velocity gradient evolution in turbulence using recent-deformation mapping of initially gaussian fields. *Journal of Fluid Mechanics*, 804:387–419, 2016.

RH Kraichnan. Rh kraichnan, phys. fluids 11, 945 (1968). *Phys. Fluids*, 11:945, 1968.

Fredrik Lundell, L Daniel Söderberg, and P Henrik Alfredsson. Fluid mechanics of papermaking. *Annual Review of Fluid Mechanics*, 43:195–217, 2011.

Charles Meneveau. Lagrangian dynamics and models of the velocity gradient tensor in turbulent flows. *Annual Review of Fluid Mechanics*, 43:219–245, 2011.

Jean-Pierre Minier et al. Probabilistic approach to turbulent two-phase flows modelling and simulation: theoretical and numerical issues. *Monte Carlo Methods and Applications*, 7 (3/4):295–310, 2001.

Ryan C Moffet and Kimberly A Prather. In-situ measurements of the mixing state and optical properties of soot with implications for radiative forcing estimates. *Proceedings of the National Academy of Sciences*, 106(29):11872–11877, 2009.

PH Mortensen, HI Andersson, JJJ Gillissen, and BJ Boersma. Dynamics of prolate ellipsoidal particles in a turbulent channel flow. *Physics of Fluids*, 20(9):093302, 2008.

Magdalena M Musielak, Lee Karp-Boss, Peter A Jumars, and Lisa J Fauci. Nutrient transport and acquisition by diatom chains in a moving fluid. *Journal of Fluid Mechanics*, 638: 401–421, 2009.

Rui Ni, Nicholas T Ouellette, and Greg A Voth. Alignment of vorticity and rods with lagrangian fluid stretching in turbulence. *Journal of Fluid Mechanics*, 743, 2014.

Alain Pumir and Michael Wilkinson. Orientation statistics of small particles in turbulence. *New journal of physics*, 13(9): 093030, 2011.

Lilach Sabban and René van Hout. Measurements of pollen grain dispersal in still air and stationary, near homogeneous, isotropic turbulence. *Journal of Aerosol Science*, 42(12): 867–882, 2011.

Mansoo Shin and Donald L Koch. Rotational and translational dispersion of fibres in isotropic turbulent flows. *Journal of Fluid Mechanics*, 540:143–173, 2005.

Dario Vincenzi. Orientation of non-spherical particles in an axisymmetric random flow. *Journal of Fluid Mechanics*, 719: 465–487, 2013.

Michael Wilkinson and HR Kennard. A model for alignment between microscopic rods and vorticity. *Journal of Physics A: Mathematical and Theoretical*, 45(45):455502, 2012.

Haifeng Zhang, Goodarz Ahmadi, Fa-Gung Fan, and John B McLaughlin. Ellipsoidal particles transport and deposition in turbulent channel flows. *International Journal of Multiphase Flow*, 27(6):971–1009, 2001.